INFN-Pisa/AE 93/17
September 27,1993

Behaviour of Microstrip Gas Chamber in strong magnetic field

F.Angelini, R.Bellazzini, A.Brez, M.M.Massai, R.Raffo, G.Spandre, M.Spezziga
INFN-Pisa and University of Pisa
Pisa, Italy
M.Bozzo
INFN-Genova and University of Genova
Genova, Italy
T.Meyer, R.Ribeiro
CERN, European Organization for Nuclear Research
Geneva, Switzerland
A.Markou
NRCPS Democritos, Attiki
Athens,Greece
J.F.Clergeau, D. Contardo, G.Smadja
IPN Lyon and Universite' Claude Bernard-ISM
Lyon, France

Abstract

The behaviour of the Microstrip Gas Chamber has been studied in strong magnetic fields (up to 2.3 Tesla). An almost complete compensation of the effect due to the **ExB** factor, which is otherwise responsible for a degradation of the spatial resolution, has been obtained by applying a small tilt to the chamber equal to the Lorentz angle. Different gas mixtures have been studied: an improvement in the resolution has been achieved using gas mixtures with higher cluster density (DME-CO_2, DME-CF_4).

Paper submitted for publication in Nuclear Instruments and Methods A

UNIVERSITÀ DEGLI STUDI DI PISA

DIPARTIMENTO DI FISICA

Istituto Nazionale di Fisica Nucleare

Sezione di Pisa

1. Introduction

The resolution, speed, granularity and radiation hardness requested for the inner tracking system for the next generation of high luminosity hadron colliders (LHC / SSC) is one of the present great challenges in the detector design . The Microstrip Gas Chamber has demonstrated to offer these attractive features as tracking detector [1-5], so that almost all the proposed future experiments (CMS,ATLAS,SDC) include the MSGCs in their central tracking system [6,7]. Nevertheless, the presence of a very intense, solenoidal, magnetic field (up to 4 T in the case of the CMS spectrometer), is common to all these experiments. The field, though necessary for best momentum analysis, could lead to a degradation of the detector performance. Indeed, a Lorentz term **ExB** changes the direction of drift of the ionisation electrons by an angle α_L, given approximately by the ratio of magnetic to electric force ($\text{tg}\,\alpha_L \approx |\mathbf{v_D x B}|/E$). Hence the primary charge is spread over a larger number of microstrip cells and this results into a displacement of the charge centroid and into a worsening of the spatial resolution and detection efficiency. From a phenomenological point of view the problem is identical to the detection of a track inclined of an angle α_L with respect to the normal to the detection plane. This effect becomes more pronounced when the electric field is orthogonal to the magnetic field as in the case of the barrel part of the CMS tracking system. To study quantitatively this effect an extensive experimental study of the behaviour of the MSGC in magnetic field has been carried on using the RD5 magnet at the CERN SPS. The possibility to compensate the worsening of the spatial resolution by means of a small tilt of the chambers and a proper choice of the gas mixture was also studied.

2. Experimental set-up

The test has been performed at the CERN SPS with a 300 GeV/c μ^- beam.

A telescope made of two standard MSGC's of the type already used in the NA12 experiment [4] and one MicroGap Chamber [8] was installed within the RD5 superconducting solenoid in a position where the maximum field intensity could reach 2.24 Tesla. A silicon microstrip telescope was used as external position reference system. In the trigger a small 2x2 cm^2 counter defined a beam spot of the size of the Microstrip Chambers. A fourth MSGC, out of the beam, was illuminated with a Fe^{55} source to provide a continuous monitor of the gas gain. The MSGCs on the beam had the strips oriented parallel to the magnetic field, while the drift field was orthogonal to **B.** The chambers were mounted on special supports which could rotate around an axis parallel to the magnetic field to study the compensation of the Lorentz angle. A schematic view of the experimental set-up is shown in fig 1.

Two MSGCs were mounted back to back on the same rotating frame. In this case the drift field **E** had equal direction but opposite sign in the two chambers. The shift of the charge centroid due to the **ExB** term is in opposite direction in the two chambers (see fig 2). The observed overall displacement was therefore amplified by a factor two, hence better detected. Two Hall

probes positioned at the beginning and at the end of the MSGC telescope were used to measure the intensity of the magnetic field. During the test run three gas mixtures were used (Argon -DME, DME-CO_2 and DME-CF_4). These gas mixtures were chosen for their high ionization density, fast drift velocity and small diffusion coefficient, factors which should provide high resolution and full detection efficiency in the thin detectors which have to be used at LHC/SSC.

3. Experimental results

The fast read-out chain used in this test is the same already used with a similar set-up in the Na12 experiment [4]. The delta current response of the shaping amplifier (Laben 5185) was adjusted to have 10 ns rise-time and 50 ns width (FWHM).

The microstrip anode signals were recorded individually by means of LeCroy 2282 ADC, while the cathode signals were read-out in groups of sixteen. For each chamber a simple cluster algorithm allowed to determine the charge cluster produced by the particle, whose coordinate was then computed with the center of gravity method. At B=0 the relative alignment of the three chambers was evaluated by computing the position differences between each pair of chambers. The difference between the measured and the expected coordinate in the 3rd chamber as derived from the first two MSGCs is computed according to the relation :

$$1) \quad \Delta Y = Y_3 - \{ Y_2 \cdot (1 + L_{23}/L_{12}) - Y_1 \cdot L_{23}/L_{12} \}$$

where L_{23} =43 mm and L_{12}=50 mm are the chambers distances. The spatial resolution was then estimated from the r.m.s. width of the distribution of the track residuals in the 3rd chamber. Assuming the position resolutions of the three chambers $\sigma_1 \approx \sigma_2 \approx \sigma_3$, the average resolution is given by :

$$2) \quad \sigma^2 = \sigma^2_{\Delta Y} / \{ 1 + (1 + L_{23}/L_{12})^2 + (L_{23}/L_{12})^2 \} = (\sigma_{\Delta Y}/2.28)^2$$

At B≠0 the displacement of the average reconstructed cluster position with respect to the case B=0 is a direct measure of the Lorentz angle α_L ($tg(\alpha_L) = \Delta Y_{av} / D$, where D is the gas gap). The contribution to ΔY due to the bending of the beam, which is nearly 0.7 mrad in the strongest magnetic field and corresponds to a shift between the first and the last chamber of 65μm, was automatically subtracted by the projective algorithm. The dependence of the Lorentz angle on the intensity of the magnetic field for different values of the electric field and different gas mixtures is shown in fig 3. The slope is almost constant (≈4°/Tesla) and no deviation from linearity was observed. The value of the drift field reported in the figure has been obtained by means of an approximate theoretical expression which gives the electric field as a function of the MSGC's geometrical parameters and working voltages in the case of substrates with a thin

resistive layer. At a distance from the detection plane greater than the pitch E_{drift} can be written as:

3) $E_{drift} = (V_d - V_{mean})/D$

where V_{mean} is the effective mean voltage at the detection plane. It is given by:

4) $V_{mean} = \{Va \cdot wa + Vc \cdot wc + (Va + Vc) \cdot w_s\}/P$

where V_a, V_c, V_d are the voltages applied respectively to anodes, cathodes and far cathode (drift electrode), w_a, w_c are the width of the anode and cathode strips, w_s is the space between cathode and anode and P the pitch.
In our specific case the expression 4) can be written as

5) $E_{drift} = (V_d - \alpha \cdot V_c)/D$, with α=0.65 for the MSGC and α=0.955 fot the MGC

Such expression has been checked by numeric computations performed with the electrostatic modeler ELECTRO [9] and found accurate within a few %.
Fig. 4 shows the ΔY distribution obtained for DME-CF_4 at B=0 and the ΔY distribution at B=2.24 Tesla. It is clearly visible the shift due to the Lorentz angle and the worsening of the spatial resolution which decreased from 34 to 94 μm.
Fig 5 shows the spatial resolution as a function of B for different drift fields and gas mixtures.
Fig 6 shows the width of the cluster, i.e. the number of strips hit, as a function of B. As it is well evident an increase in the value of α_L due to the magnetic field is reflected in a progressive loss of resolution and in a widening of the charge distribution.
A typical pulse height distribution is shown in Fig 7a. The detection efficiency, defined as the fraction of crossing tracks detected by the 3rd chamber within ± 3 σ of the residual distribution resulted greater than 99% up to 2.24 Tesla for DME-CF_4 (fig 7b). The threshold for the cluster amplitude was set at 4.5 times the r.m.s of the individual channel noise. Fig 8 shows the improvement of the resolution obtained increasing the electric field at the highest value of the magnetic field. A similar linear dependence is followed by the Lorentz angle as a function of E (fig 9).
The effect of the compensation on the resolution and on the cluster size is shown in fig 10. The system of MSGCs was rotated around an axis parallel to the magnetic field until the displacement was corrected. The minimum of the resolution for the three gas mixtures was found at $\alpha_C = 10^o \pm 0.5^o$. The major error source is systematic and is due to the rotation mechanics. The compensation angle corresponds to the Lorentz angle and results in a full recovery of the resolution measured at B=0. The best values measured for the resolution were 32μm for DME-CO_2, 34μm for DME-CF_4 and 35μm for Ar-DME. It must be stressed

that the best results were obtained with the gas mixtures of higher density. The cluster size at the compensation angle corresponds to the cluster size obtained at B=0 indicating that the effect of the magnetic field on lateral diffusion is small. Fig 11 shows the detection efficiency as function of the compensation angle. At a rotation angle equal to α_L, the efficiency of the three gases was greater than 97%. The slight decrease of efficiency for Ar-DME and for DME-CO_2 was due essentially to the lower gain at which the chambers were operated with these gases.
A "digital" algorithm was also used to derive the particle coordinate. In this case we gave to all the strips over threshold the same weight, independently of the pulse amplitude, to simulate a fast processing of the data without ADC use. For ease of comparison, in fig 12 are shown the resolutions obtained with the center of gravity method and with the digital algorithm as a function of compensation angle.
From the measurement of the Lorentz angle and from the knowledge of the magnetic and electric field intensity it is also possible to measure the drift velocity of the different gas mixtures, using the relation $v=\alpha_L E/B$. The drift speed was found comprised between 6.7 and 7 cm/μs at maximum electric and magnetic field strength. This means that the trail of ionisation electrons released by the charged muon in the 3 mm gas gap was collected at the anode in less than 50 ns.

4. Discussion and conclusions

We have studied the behaviour of Microstrip Gas Chamber in strong magnetic field. A Lorentz angle of nearly 4^o/Tesla and a drift speed of ≈ 7 cm/μs have been measured for several gas mixtures. The Lorentz angle and the drift velocity depend strongly on the electric drift field intensity. This is the major difference between MSGCs and other gas detectors like standard cylindrical proportional counters or their modern version, the straw tubes. In the straw tube one voltage sets at the same time the drift and the amplification field, while in the MSGC the drift field can be made very high (up to 10 times that one in the proportional counter) without affecting very much the amplification field. A very high drift field is essential in controlling the rise of the Lorentz angle and in providing a fast charge collection.
The measured Lorentz angle $\alpha_L \approx 10^o$ at 2.24 Tesla induces significant effects on the position resolution which worsens from ≈ 30 μm to ≈ 100 μm. The detection efficiency remains full up to the maximum B field. A full recovery of the resolution measured at B=0 is obtained by rotating the chamber at an angle equal to the Lorentz angle. The conclusion is that at least for high p_t tracks the effect of the magnetic field can be fully compensated. Further studies on the behaviour of the MSGC for inclined tracks are under way.

Acknowledgements

We want to express our gratitude to all the RD5 team for their hospitality and help.
We thank G.Decarolis, M.Favati, C.Magazzu' and S. Tolaini of INFN-Pisa for their enthusiastic technical support.

References

1) F. Angelini et al., Particle World, vol. 1 n.3 (1990) 85
2) M.H.J. Gijsberts et al., Nucl. Instr. and Meth. A313 (1992) 377
3) F.Angelini et al., INFN PI/AE 93/07 accepted for publication on Nucl. Instr. and Meth.
4) F. Angelini et al., Nucl. Instr. and Meth. A315 (1992) 21
5) RD22 Collaboration, CERN/DRDC 92-51
6) CMS Collaboration, Letter of Intent, CERN/LHCC 92-3
ATLAS Collaboration, Letter of Intent, CERN/LHCC 92-4
7) SDC Collaboration, Technical Design Report, SSCL-SR-1215
8) F. Angelini et al., INFN PI/AE 93/10, accepted for publication on Nucl. Instr. and Meth.
9) ELECTRO - I.E.S., Manitoba, Canada

Preprint request to:
R.Bellazzini
INFN-Pisa, Via Livornese 582/A
56010 S.Piero a Grado, Pisa, Italy

Table1. - Geometrical parameters of the MSGCs and operating voltages.

	MGC	MSGC2	MSGC3
Anode width (μm)	5	9	9
Cathode width (μm)	187	70	70
Pitch (μm)	200	200	200
Active area (mm^2)	25x25	25x25	25x25
Drift space (mm)	3.1	3.0	3.2
Cathode voltage(V)	-450	-700	- 700
Anode voltage (V)	0	0	0
Drift voltage (V)	- 3450	- 3500	- 3600

Figures captions

Fig 1. - A schematic view of the experimental set-up

Fig 2. - a): The principle of measurement of the Lorentz angle.
b): The compensation mechanism

Fig 3. - The dependence of the Lorentz angle on the intensity of the magnetic field for different values of the electric field and different gas mixtures

Fig 4. - The distribution of the track residuals at B=0 and B= 2.4 Tesla

Fig 5. - The spatial resolution as a function of B for different drift fields and gas mixtures

Fig 6. - The width of the cluster (number of hit strips) as a function of B

Fig 7.- a): A typical pulse height distribution
b): The detection efficiency as a function of B

Fig 8 - The spatial resolution as a function the drift field E_{drift} at the highest value of B

Fig 9. - The Lorentz angle as a function of E_{drift} at the highest value of B

Fig 10. - a): The spatial resolution as a function of the tilt angle of the MSGCs
b): The cluster size as a function of the tilt angle of the MSGCs

Fig 11. - The detection efficiency as a function of the tilt angle of the MSGCs

Fig 12. - The analog and the digital position resolution as a function of the tilt angle for DME- CF_4 mixture

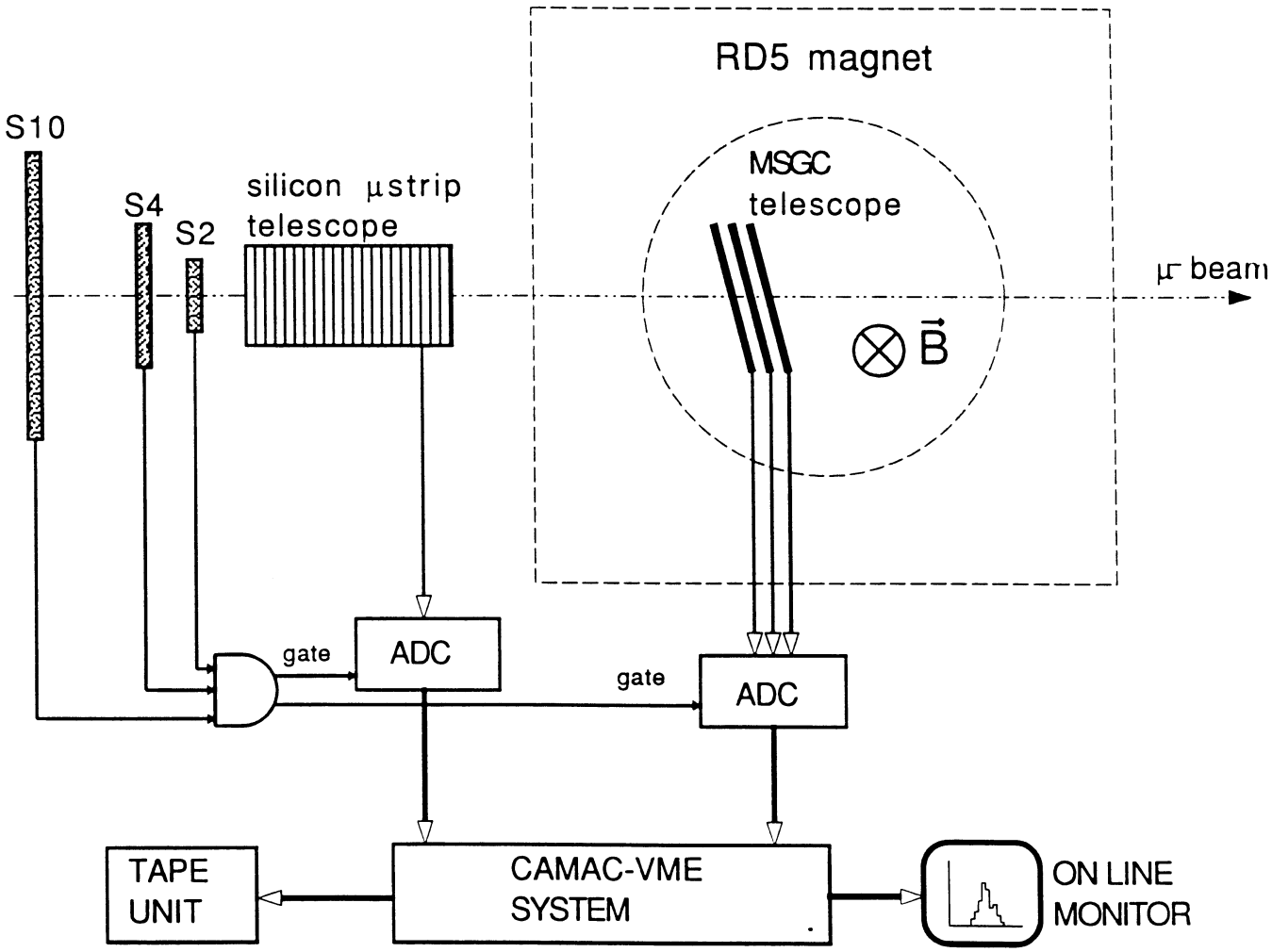

Fig 1. - A schematic view of the experimental set-up

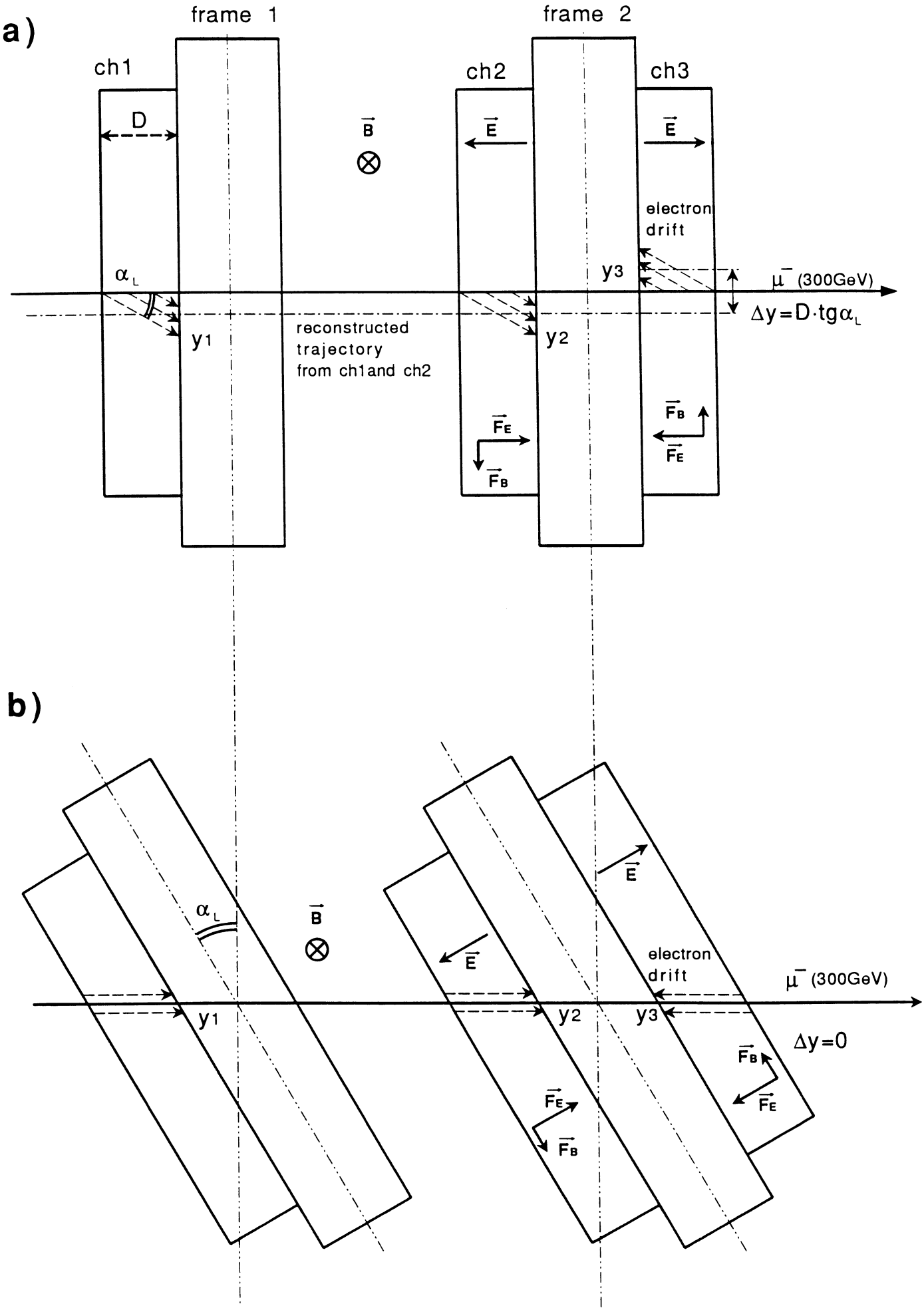

Fig 2: a) - The principle of measurement of the Lorentz angle
b) - The compensation mechanism

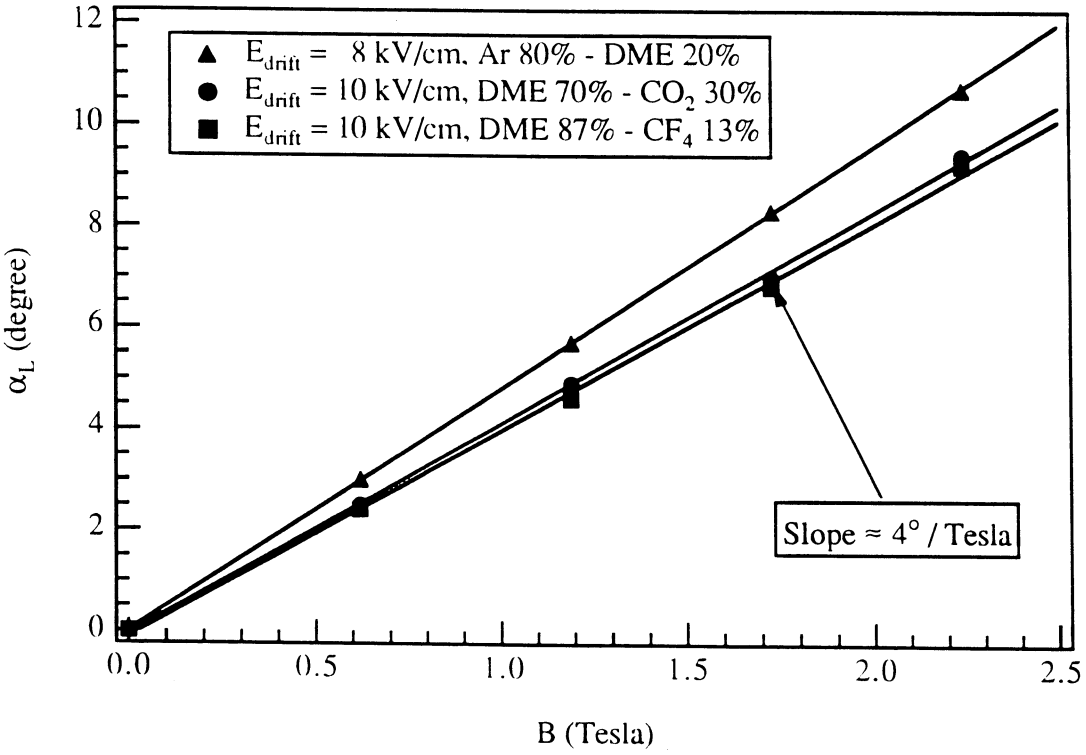

Fig 3. - The dependence of the Lorentz angle on the strength of the magnetic field for different values of the electric field and different gas mixtures

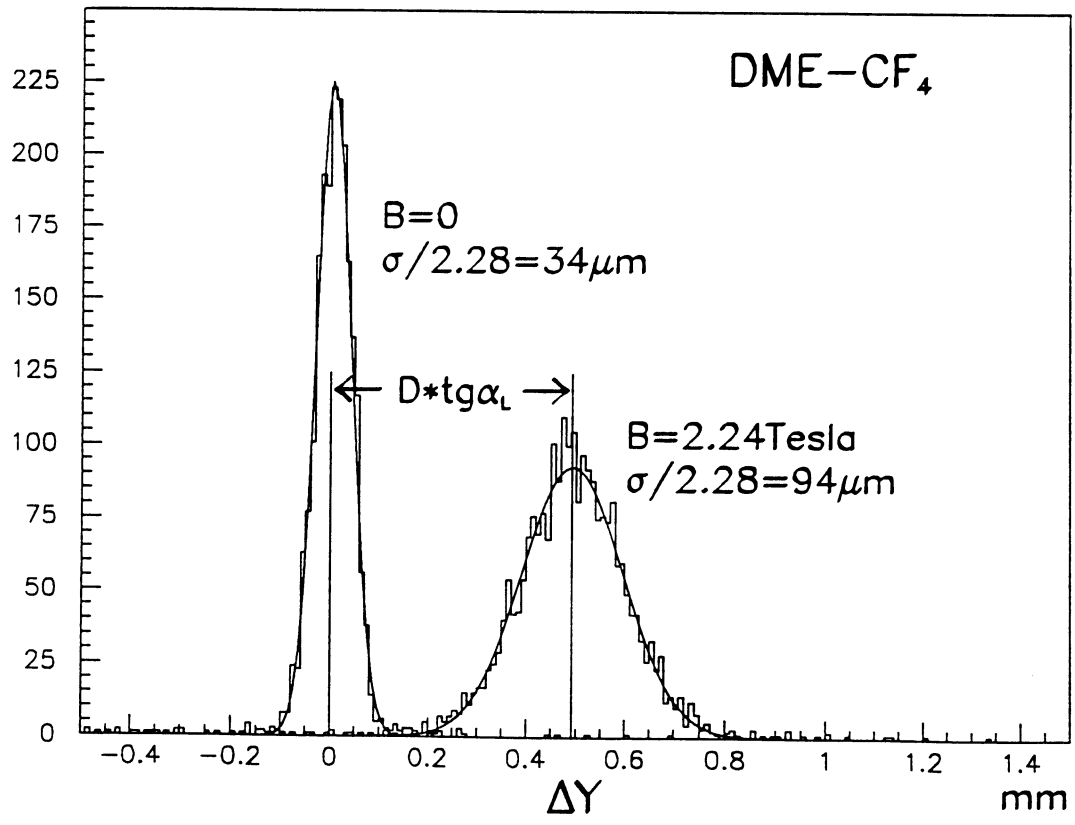

Fig 4.– The distribution of track residuals at B=0 and B=2.24Tesla

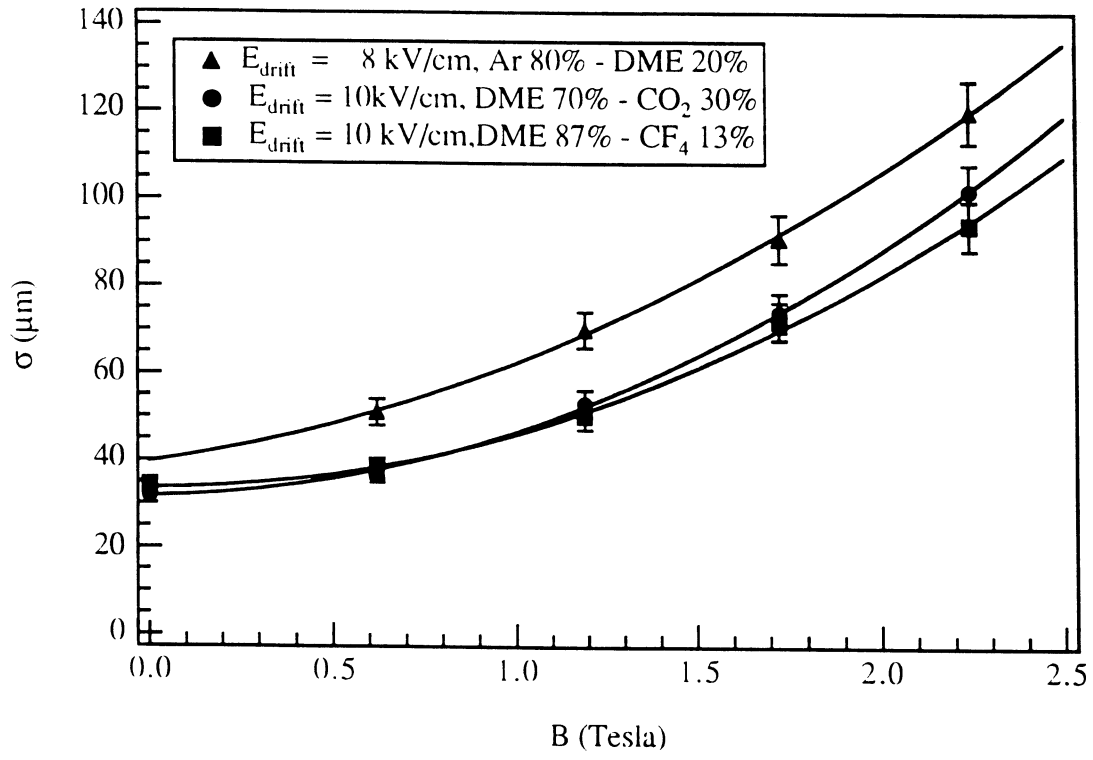

Fig 5. - The spatial resolution as a function of B for different drift fields and gas mixtures

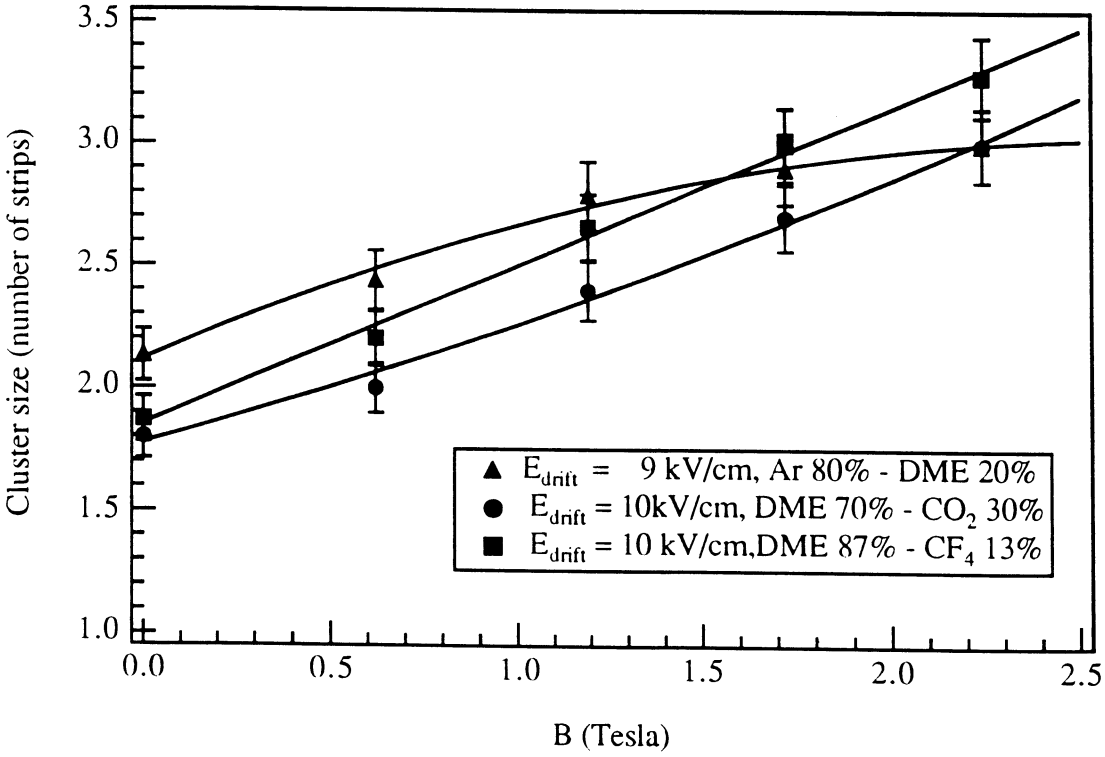

Fig 6. - The width of the cluster (number of hit strips) as a function of B

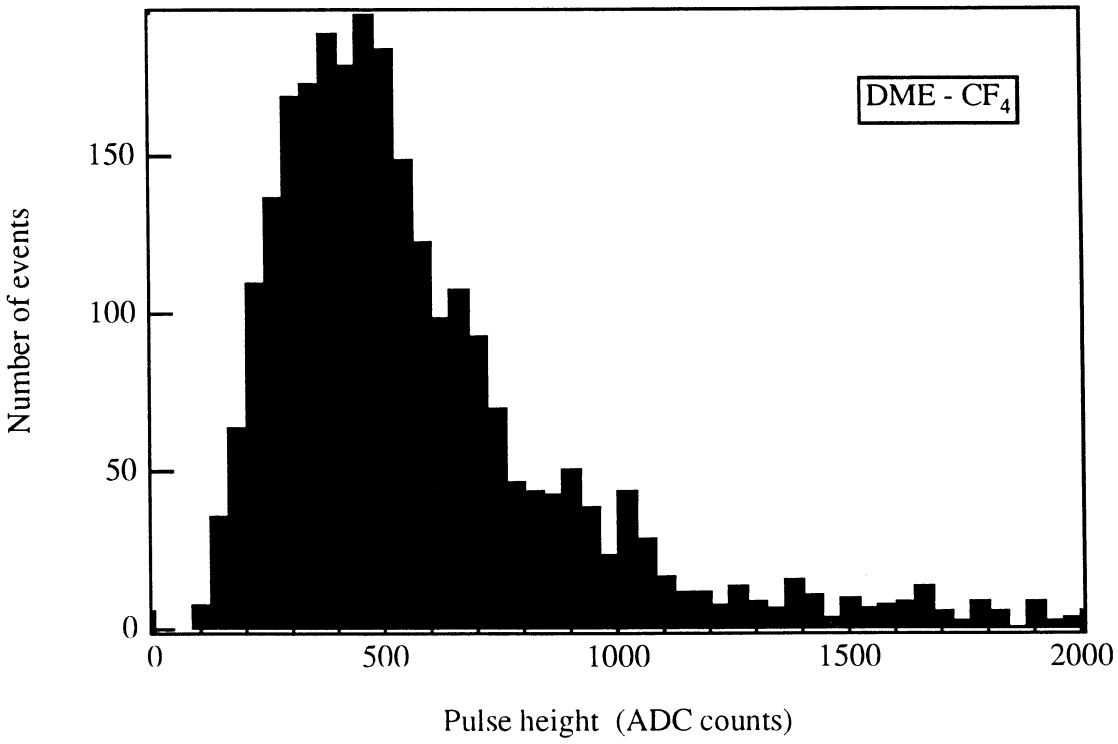

Fig 7a. - A typical pulse height distribution

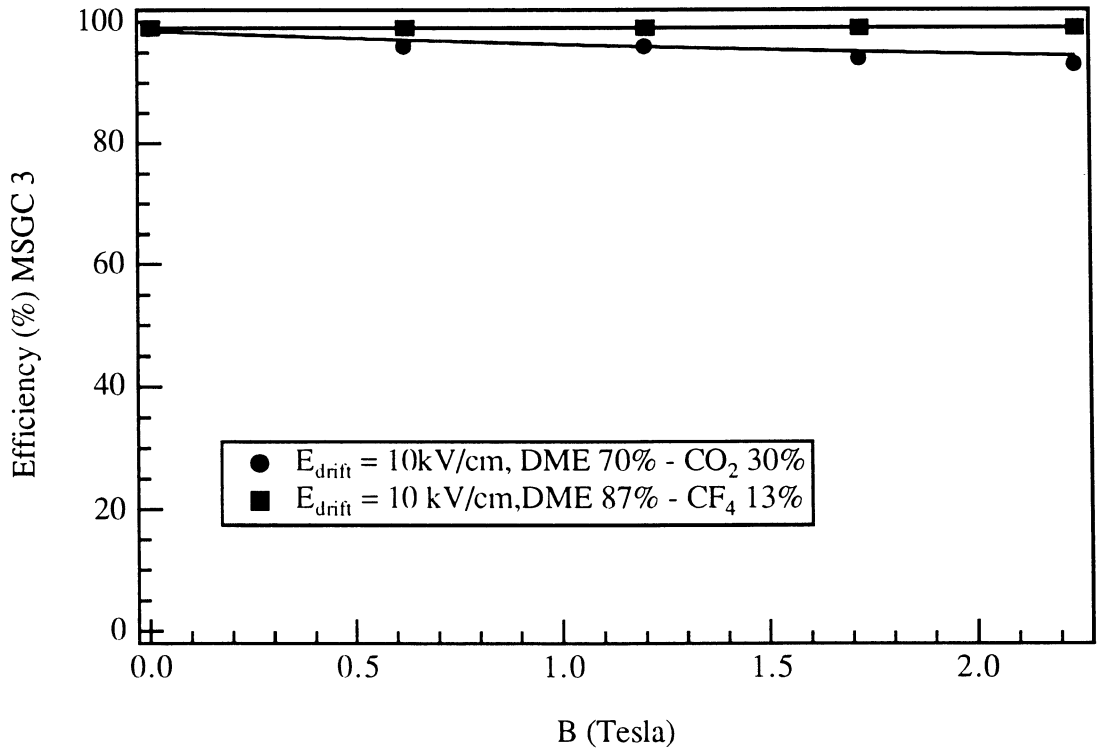

Fig 7b. - The detection efficiency as a function of B for DME-CF_4 and DME-CO_2 gas mixtures

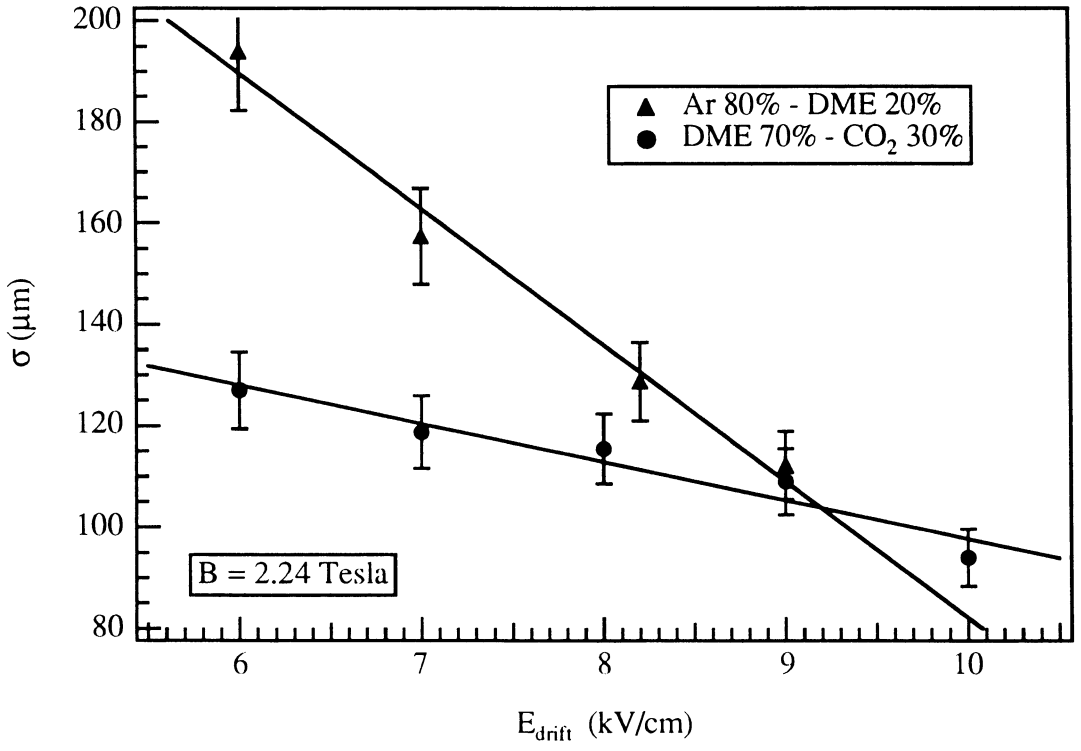

Fig 8. - The spatial resolution as a function of the drift field at the highest value of B

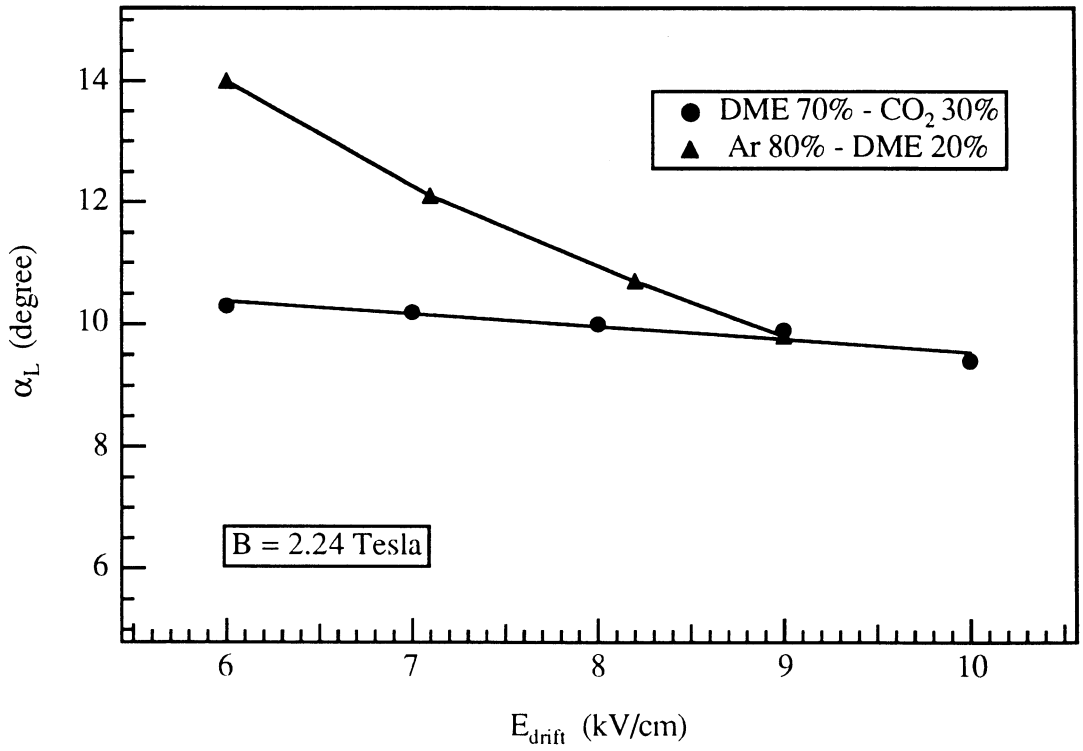

Fig 9. - The Lorentz angle as a function of E_{drift} at the highest value of B

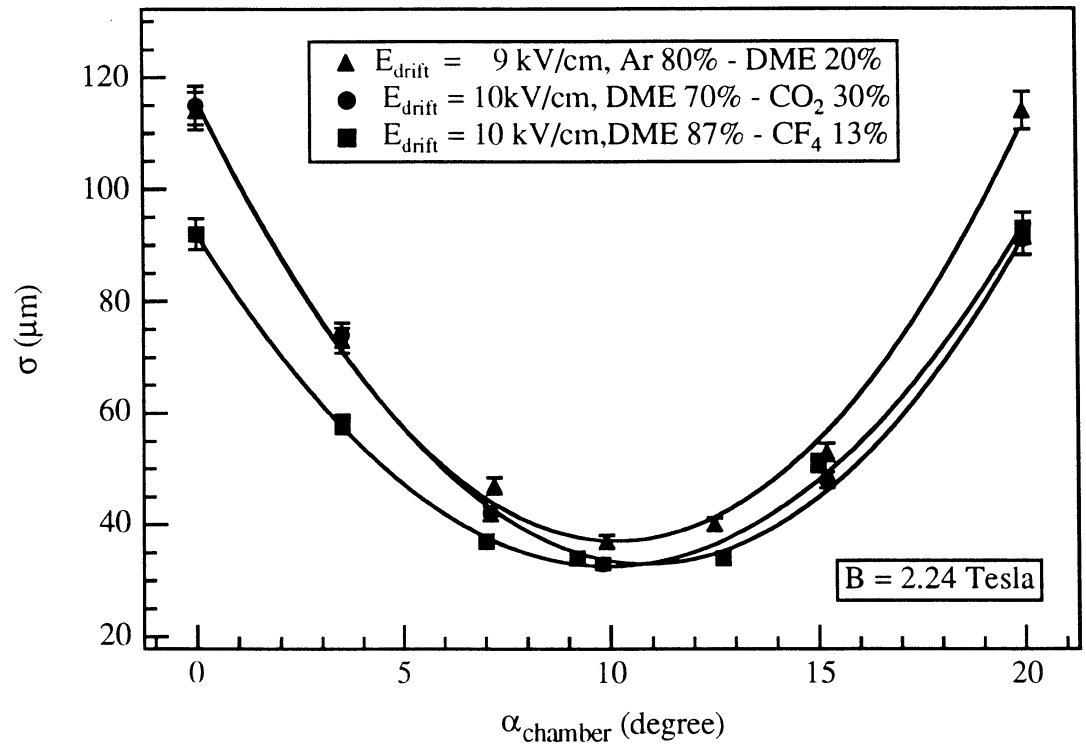

Fig 10 a. - The spatial resolution as a function of the tilt angle of the MSGCs

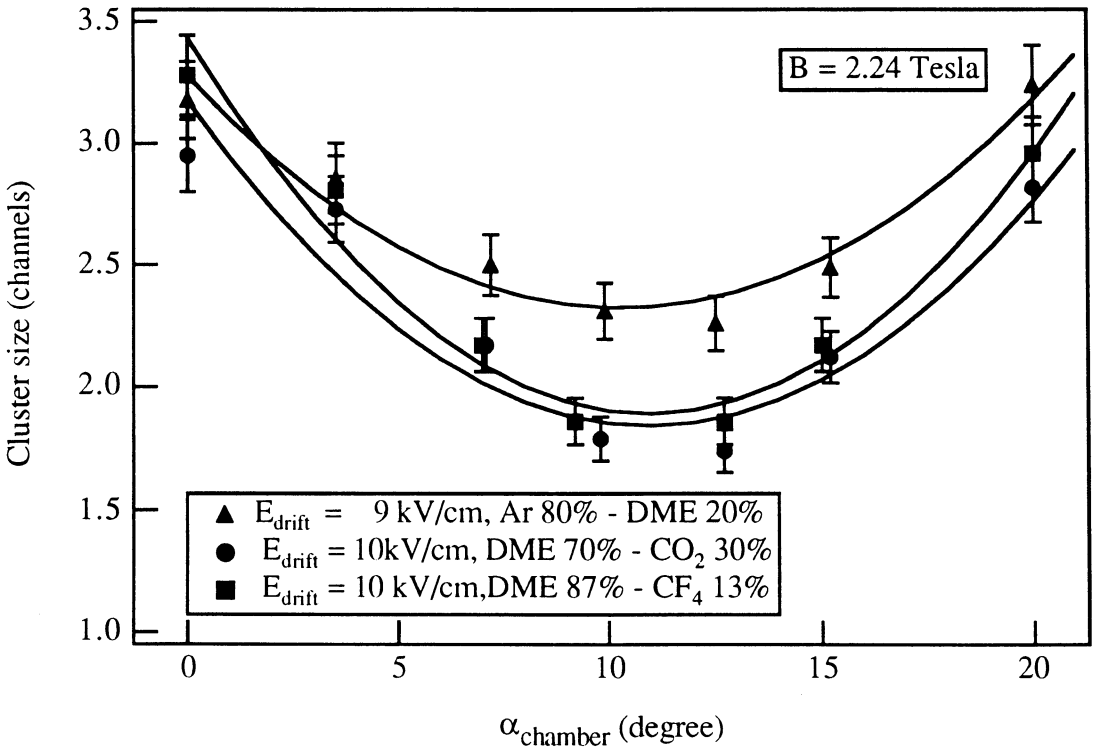

Fig 10 b. - The cluster size as a function of the tilt angle of the MSGCs

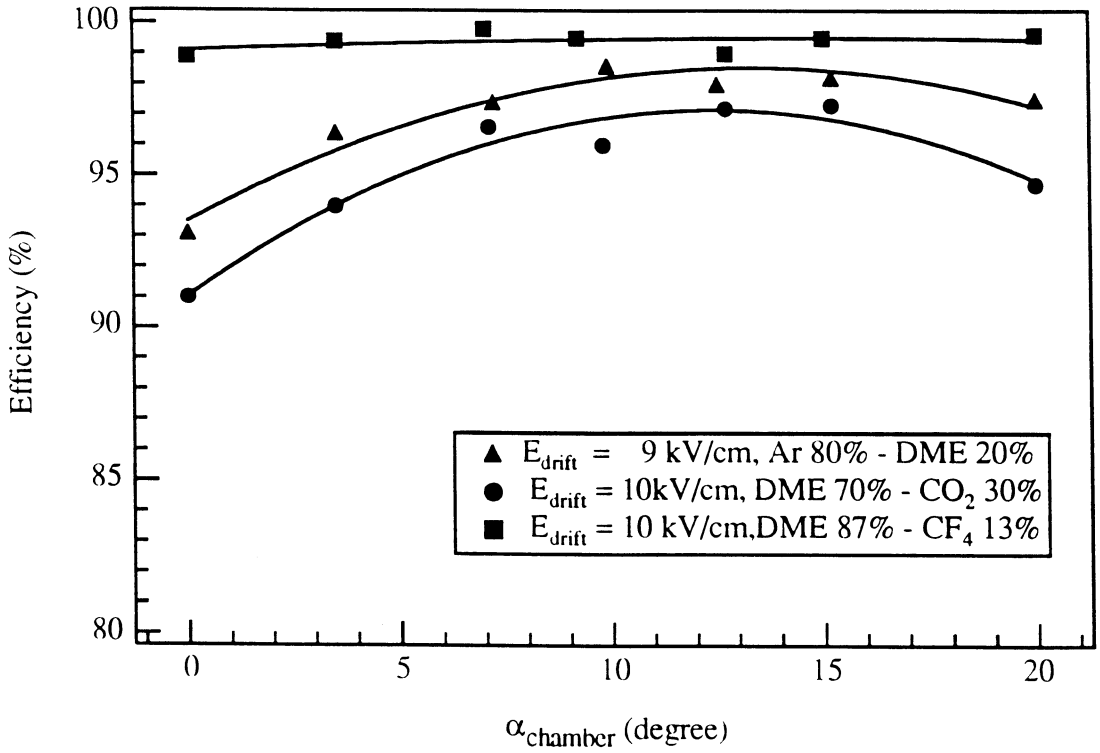

Fig 11. - The detection efficiency as a function of the tilt angle of the MSGCs

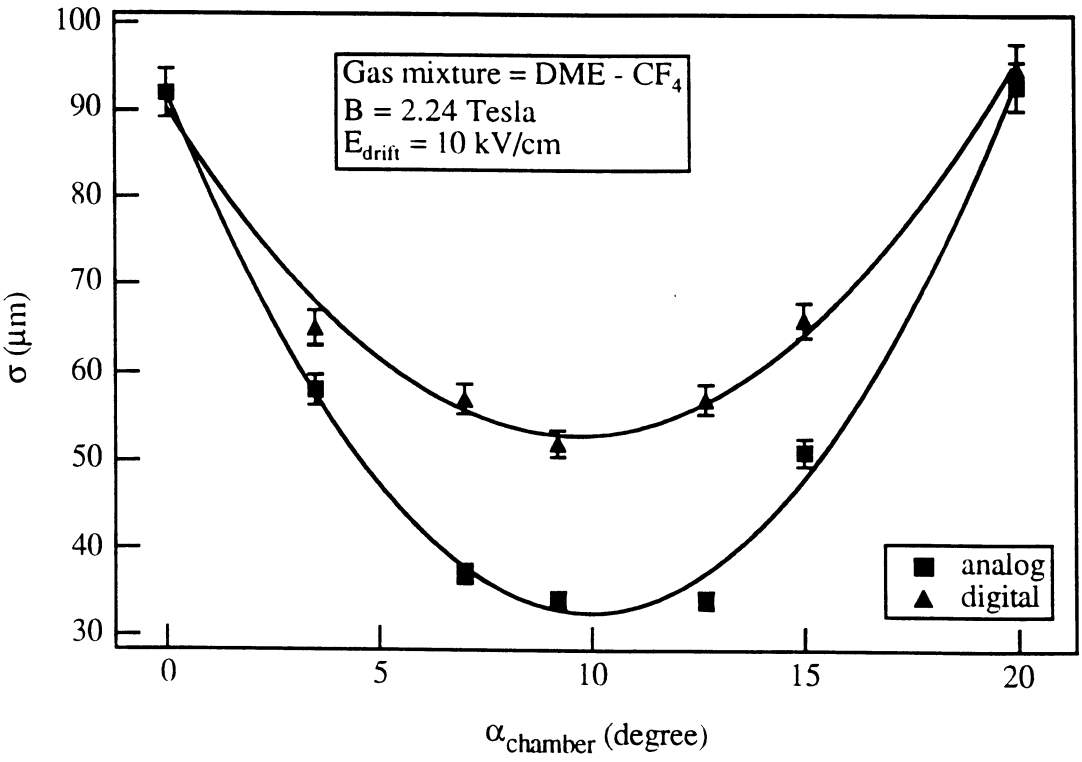

Fig 12. - The analog and digital position resolution as a function of the tilt angle for DME-CF_4 mixture